PRODUCTION OF BIOFUELS USING HYDROLYSIS AND FERMENTATION

J.P.F. Charpin[*], A.D. Fitt[†], H. Laurie[‡], H. Mambili,
A. Ouhinou, A. Oomykala and L.Uys

Workshop participants
N. Fowkes, G. Fargo and L. Lishiuha

Industry representative
S. Van Zyl

Abstract

Models are developed to study the production of ethanol from cellulose using hydrolysis and fermentation. The chemical reactions are simulated using two different models: a crude model useful for engineering design, and a more accurate enzyme dynamics model useful for biochemical investigations. The results obtained by the two models are consistent with each other and available results. Both show that the concentration of cellulose decays exponentially. The fluid flow in the production tank was also considered. Cellulose particles need to remain in suspension in the production tank. This is achieved using an impeller. Simple fluid dynamics models were developed to assist with its design. The settling velocity of the particles is expressed using standard Stokes' law, and Newton's second law. It varies with the cellulose concentration in the tank. A study of the liquid flow in the tank provides minimum mixing conditions.

1 Introduction and problem specification

In recent years, biofuels have been developed to become an alternative to fossil fuels. Numerous solutions are being investigated [1] and bioethanol is one of the

---

[*]Department of Mathematics and Statistics, University of Limerick, Ireland *email: jean.charpin@ul.ie*

[†]Pro Vice-Chancellor (Research and Knowledge Transfer), Oxford Brookes University, Headington Campus, Gipsy Lane, Oxford 0X3 0BP, United Kingdom. *email: afitt@brookes.ac.uk*

[‡]Deaprtment of Mathematics and Applied Mathematics, University of Cape Town, Rondebosch 7701. *email: henri.laurie@uct.ac.za*

most popular ones. The switch towards this fast developing biofuel is promoted and encouraged by governmental policies in the United States, the European Union and South America [2, 3, 4]. The production and economy of bio-ethanol is therefore subject to intense investigation.

Bio-ethanol may be produced from feedstocks containing sucrose, starch or lignocellulosic biomass [2, 5]. The first generation of bio-ethanol uses food crops such as maize or sugar cane [6]. To this day, sugar crops are the most productive feedstocks [7] and the production of this type of bio-ethanol has reduced the dependence on fossil fuels [6]. Unfortunately, this source of bio-ethanol generates a strong competition with food production [3]. The economical choice 'food vs fuel' causes controversy and leads to very serious debate [8, 9]. Alternative sources for the production of bio-ethanol should therefore be found: the second generation of bio-ethanol is produced from lignocellulose feedstocks such as bagasse, straw, corn stover wood waste or agricultural waste [6]. Although they compete as well with other resources such as animal feed or electricity production [10], these cellulosic feedstocks are the most abundant [7] and in the long term they will have to be favoured [3, 10].

Once harvested, the raw materials are processed and transformed to sugar and then to ethanol using a three stage process:

1. Pre-treatment
   Cellulose is converted to sugar first. This is a slow transformation that can be sped up if a pre-treatment is applied. Numerous methods can be applied depending of the raw material [3]. They include mechanical processing, treatment with different types of acids, alkaline hydrolysis, steam explosion, ammonia fibre expansion (AFEX) or various forms of oxidation [5, 10, 11].

2. Hydrolysis and fermentation
   During this second stage, the cellulose is transformed to ethanol in several steps, using enzymes and fermenting organisms. Lignocellulosic raw materials used for second generation bio-ethanol are also harder to ferment to ethanol [3]. Higher temperatures and specifically engineered fungal/bacterial strains are currently researched to overcome this difficulty [6].

3. Finally, ethanol must be recovered

Like fossil fuels, bio-ethanol has a non-negligible environmental cost. The complete cycle from the harvesting of raw materials, the transport and production processes and the final combustion leads to an energy balance favourable to bio-ethanol but can result in environmental degradation in the form of soil acidification and toxicity is not always positive [7]. Also in spite of improvements, the production of bio-ethanol still generates a significant amount of greenhouse gases [12]. Each stage of the process is therefore under intense investigation [6, 13, 14].

Numerous studies have focused on improving the production of biofuels by enzymatic hydrolysis of cellulose to glucose and subsequent fermentation to ethanol. In particular a more efficient conversion of cellulose to glucose could significantly reduce production costs; the models developed here may assist with this process. Some mathematical models have been proposed to help study this problem. Among these models there is a large set of empirical models (amongst others, see [15, 16, 17]), which help in understanding various properties of different substrate and enzymes and their interactions during the process, as well as estimating the different rates of reactions. Another set, such as [18, 19], develop deterministic mathematical models of this complex process.

Using a practical population model combined with reaction kinetics, South et al [18] predict the conversion of the substrate over a four-fold range of enzyme loadings and more than ten-fold range of substrate. The authors proposed a kinetic model to predict the simultaneous saccharification and fermentation of insoluble cellulose. On closer inspection their model has some anomalous properties, for example, the model does not conserve mass and generates negative solutions. The model allows ethanol to inhibit yeast growth, a high concentration (that is, some value greater than a threshold [18]) will lead to decay of the yeast population. In reality, once ethanol is produced it is not consumed or used by any of the other components, hence can only increase monotonically or reach a stable plateau when there is no longer production. The model proposed by South *et al.* [18] overcome this deficiency by allowing the rate of ethanol production to follow that of the yeast population, potentially breaking the monotony of ethanol production.

This model was later modified by Shao et al. [19], to accommodate intermittent feeding of substrate and enzyme. It was found that cellulose conversion increases with decreasing feeding frequency. Their modification of the [18] model preserves the positivity of solutions. However, it still shares the other problems of the South et al. model [18].

A new hydrolysis and fermentation method is currently investigated at the Centre of Renewable and Sustainable Energy Studies in the University of Stellenbosch in South Africa. Cellulose particles are mixed with enzymes and yeast in a fermentation tank. After approximately five days of chemical reactions, most of the cellulose has been converted to ethanol. The process is currently being tested in a small tank but the team is considering the difficulties of using the same method at industrial level: ultimately, the process will take place in a $1000m^3$ cylinder, 9m in diameter and 18m high. The cellulose particles are typically wooden spheres of 1mm in diameter. They are introduced at the top of a tank where enzyme and yeast are well mixed with a nutrient rich solution. The particles start falling straight away. To prevent a build up at the bottom of the tank an impeller will be installed. This aspect of the production process raised some mathematical difficulties and the problem was

presented at the seventh South African Mathematics in Industry Study Group in Industry (MISGSA) held in Cape Town in January 2010. The rate of mixing is much faster than the reaction rates of the process. Mixing typically occurs within seconds while the biological reactions take days. The objective of the present study is to guarantee that the particles are well mixed in the fluid at any point in time so the chemical reaction occurs in optimal conditions at any point in time during the production.

Models were developed for two different aspects of the problem:

- **Chemical reactions.** The cellulose is mixed in with three types of enzymes and yeast in water. Ethanol is then produced after three chemical reactions and one fermentation step. Two sets of equations will be presented to study the variation of concentrations in the mixture: a simplified set will first be considered and a system describing the reactions in more detail will be presented. This aspect will presented in Section 2.

- **Fluid mechanics.** At the beginning of the production process, cellulose is introduced in the form of small particles at the top of a huge tank. They are mixed with water, yeast and enzymes using an impeller located close to the bottom of the tank. When the impeller is stopped, the particles start falling down. This will slow down the reactions and after some time, the impeller has to be started again. The movements of the particles are studied in Section 3. The movement of the fluid and particles is also briefly studied when the impeller is switched on.

2   Chemical reactions

The reactions involved in the breakdown of cellulose and the subsequent fermentation of the breakdown products is shown in Figure 2. Cellulose is a polymer that is broken down by an enzyme called exocellulase to form the disaccharide cellobiose. Cellobiose in turn is hydrolysed to two glucose molecules. Fermentation, by the micro-organism yeast, uses glucose to produce ethanol and carbon dioxide.

As a first approximation a basic kinetic model is presented in Section 2.1. This model ensures that all mass in the system is conserved and is well-posed. A more complete model is introduced in Section 2.2.

2.1   Simplified model

In this section, a simple model describing the process of cellulose breakdown and fermentation to ethanol is investigated. To start with, the tank is fed with a given

$$\left\{ (C_6H_{10}O_5)_n + H_2O \xrightarrow{\quad\boxed{1}\quad} (C_6H_{10}O_5)_{n-2} + C_{12}H_{22}O_{11} \right\}$$

$$2 \cdot C_6H_{10}O_5 + H_2O \xrightarrow{\quad\boxed{1}\quad} C_{12}H_{22}O_{11}$$

Exocellulase

$$C_{12}H_{22}O_{11} + H_2O \xrightarrow{\quad\boxed{2}\quad} 2 \cdot C_6H_{12}O_6$$

Cellobiase

$$C_6H_{12}O_6 \xrightarrow{\quad\boxed{3}\quad} 2 \cdot C_2H_5OH + 2 \cdot CO_2$$
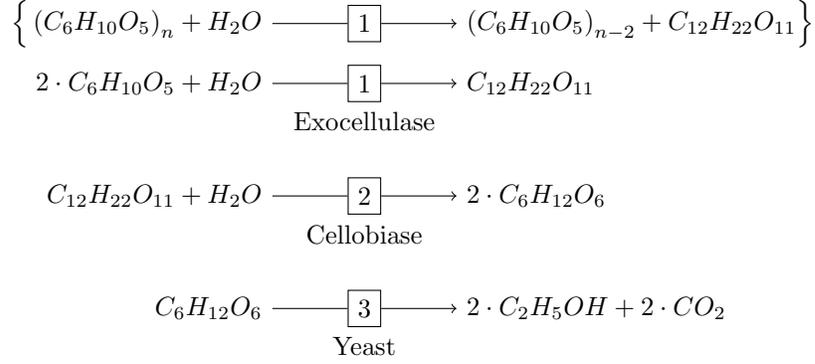
Yeast

Figure 1: Chemical reactions and fermentation step showing the conversion of cellulose to ethanol.

mass of cellulose and yeast. Small concentrations of cellobiose, glucose and ethanol may be present, they are negligible initially. The system is closed and there is no loss or gain of mass. Cellulose concentration levels is converted to cellobiose with rate constant k_1 and cellobiose is converted to glucose with a constant of k_2. All conversions and fermentations follow a mass-action law. Ethanol and carbon dioxide are produced in equimolar amounts, however because the molar masses are approximately 46 and 44 (g/mol) respectively, we further assume that the mass of ethanol produced is approximately equal to that of carbon dioxide. A proportion of the consumed glucose is used for the growth of the yeast population, in other words there is an accretion of yeast biomass. A high ethanol concentration is detrimental to yeast and inhibits growth. The dynamics of the conversion of cellulose to ethanol can therefore be formulated into the following system of ordinary differential equations,

$$\begin{aligned}
\dot{s_1} &= -k_1 s_1 \\
\dot{s_2} &= k_1 s_1 - k_2 s_2 \\
\dot{s_3} &= k_2 s_2 - k_3 s_3 y \\
\dot{s_4} &= \alpha_1 k_3 s_3 y \\
\dot{y} &= \alpha_2 k_3 s_3 y \left(1 - \frac{s_4}{K}\right) \\
\dot{s_5} &= \alpha_3 k_3 s_3 y + \alpha_2 k_3 s_3 y \frac{s_4}{K},
\end{aligned} \tag{1}$$

where k_3 is the fermentation rate constant of glucose to ethanol. The yeast make use of an amount $k_3 s_3 y$ of the available glucose. The proportion α_1 is converted to ethanol, a second part α_2 is converted to yeast biomass and the remaining

Parameter		Value
k_1	Cellulose breakdown	0.03 hours^{-1}
k_2	Cellobiose generation	0.3 hours^{-1}
k_3	Conversion to ethanol	2 hours^{-1}
$\alpha_2 k_3$	Yeast growth	0.4 hours^{-1}
α_1	Glucose to ethanol conversion rate	0.4
α_2	Glucose to yeast biomass conversion rate	0.2
α_3	Glucose to carbon dioxyde conversion rate	0.4
s_1	Cellulose concentration	g·L^{-1}
s_2	Cellubiose concentration	g·L^{-1}
s_3	Glucose concentration	g·L^{-1}
s_4	Ethanol concentration	g·L^{-1}
s_5	Carbon dioxide concentration	g·L^{-1}
y	Yeast concentration	g·L^{-1}

Table 1: Typical values for the simplified model

part α_3 represents the carbon dioxide produced. K is the threshold value beyond which the yeast dies out, the value of $K \approx 50 \ g/L$ is used in the following [18]. Typical parameter values are given in Table 1. These values were estimated from [18], with the exception of $k_1 = 0.03$. This value was adjusted to ensure that the decay of cellulose occurs over approximately 120 hours (5 days) in line with experimental observation.

Numerical solutions are shown in Figure 2. Cellulose can be seen to decrease exponentially (note the straight line on the log axis). Initially there is a rapid increase in cellobiose and glucose production which drives the production of ethanol and yeast population growth. Ethanol approaches a steady state and the supply of glucose decreases, which stops yeast growth. The system seems to approach a steady-state with a near complete conversion of cellulose to ethanol and carbon dioxide.
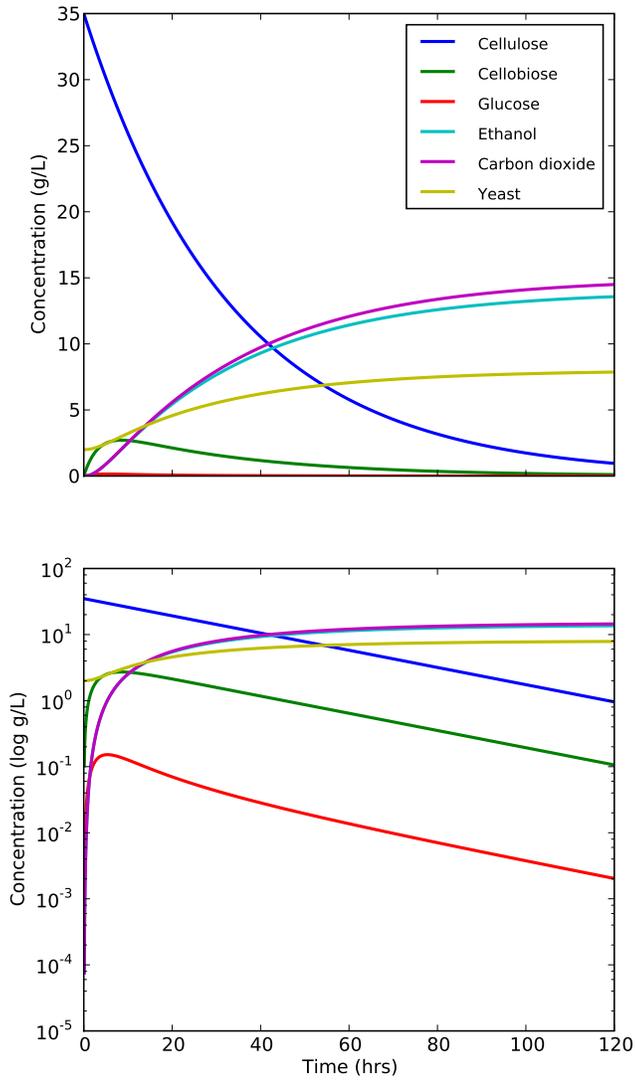
Figure 2: Time simulation showing the conversion of cellulose to ethanol via enzymatic hydrolysis and yeast fermentation over a five day period.

2.2   General system

A more advanced set of equations may be written as

$$\frac{d[CE]}{dt} = (1 + \sigma_C)\frac{d[C]}{dt} + \left[k_{fc}(1 + \sigma_C)[C][E] - \frac{k_{fc}}{K_C}[CE] \right] , \tag{2}$$

$$\frac{d[E]}{dt} = -\frac{\sigma_c}{1 + \sigma_c}\frac{d[CE]}{dt} , \tag{3}$$

$$\frac{d[C]}{dt} = -\left\{ k\left(\frac{[C]}{[C]_0}\right)^n + c \right\} \frac{[CE]}{1 + \sigma_C} \frac{K_{C/Cb}}{[Cb] + K_{C/Cb}} \frac{K_{C/Eth}}{[Eth] + K_{C/Eth}} , \tag{4}$$

$$\frac{d[Cb]}{dt} = -1.056\frac{d[C]}{dt} - \frac{K_{Cb}[Cb][B]}{[Cb] + K_m\left(1 + [G]/K_{Cb/G}\right)} , \tag{5}$$

$$\frac{d[X]}{dt} = \frac{\gamma_{max}[X][G]}{[G] + K_G}\left(1 - \frac{[Eth]}{K_{X/Eth}}\right) , \tag{6}$$

$$\frac{d[G]}{dt} = -1.053\left[1.056\frac{d[C]}{dt} + \frac{d[Cb]}{dt}\right] - \frac{1}{Y_{X/G}}\frac{d[X]}{dt} , \tag{7}$$

$$\frac{d[Eth]}{dt} = \frac{Y_{Eth/G}}{Y_{X/G}}\frac{d[X]}{dt} , \tag{8}$$

where the notation may be found in Table 2 and the constants are defined in Table 3

Parameter	Concentration
$[CE]$	Cellulose enzyme complex
$[B]$	β-Glucosidase
$[C]$	Cellulose
$[E]$	Enzyme
$[Cb]$	Cellubiose
$[X]$	Cells (Yeast)
$[G]$	Glucose
$[Eth]$	Ethanol

Table 2: Definition of concentrations

Parameter	Value	Unit
k_{fc}	1.8366	$\text{l·g}^{-1}\text{·h}^{-1}$
k	0.8359	h^{-1}
n	5.3	
c	0.18125	h^{-1}
K_{Cb}	640	h^{-1}
K_G	0.05	g·l^{-1}
K_C	1.82	l·g^{-1}
K_L	0.807	l·g^{-1}
K_m	10.56	g·l^{-1}
$K_{Cb/G}$	0.62	g·l^{-1}
$K_{C/Cb}$	5.85	g·l^{-1}
$K_{C/Eth}$	50.35	g·l^{-1}
$K_{X/Eth}$	50.0	g·l^{-1}
σ_c	0.806	
γ_{max}	0.4	h^{-1}
$Y_{X/G}$	0.09	
$Y_{Eth/G}$	0.47	

Table 3: Definition of constants

This system of equations is quite complex. However, some basic analysis can provide an approximate solution with enough accuracy for the present study. This analysis should focus on the concentration of cellulose as this is the key element of the reaction. At the start of the process, Equations (2-4) may be simplified to

$$\frac{d[CE]}{dt} = -k \left(\frac{\overline{[C]}}{[C]_0} \right)^n [CE] + \left[k_{fc} \left(1 + \sigma_C \right) \overline{[C]}[E] - \frac{k_{fc}}{K_C}[CE] \right] , \qquad (9)$$

$$\frac{d[E]}{dt} = -\frac{\sigma_c}{1 + \sigma_c} \frac{d[CE]}{dt} , \qquad (10)$$

$$\frac{d[C]}{dt} = -k \left(\frac{[C]}{[C]_0} \right)^n \frac{[CE]}{1 + \sigma_C} , \qquad (11)$$

where $\overline{[C]}$ is the average value of cellulose concentration over the period considered. The system (9-11) leads to the following concentration for cellulose:

$$[C] = C_0 \left(1 + B(t + (e^{-At} - 1)/A) \right)^{1/(1-n)} , \qquad (12)$$

where

$$A = k\overline{[C]}^n + \sigma_C k_{fc}\overline{[C]}[C]_0 + k_{rc} \, ,$$

$$B = \frac{0.0082(n-1)k \; k_{fc}(1+\sigma_C)\overline{[C]}[C]_0}{(1+\sigma_C)\left(k\overline{[C]}^n + \sigma_C k_{fc}\overline{[C]}[C]_0 + k_{rc}\right)} \, ,$$

$$\overline{[C]} = C_0 \frac{n-1}{n-2} \frac{\left(\frac{\overline{[C]}_0}{C_0}\right)^{2-n} - 1}{\left(\frac{\overline{[C]}_0}{C_0}\right)^{1-n} - 1} \, , \qquad \overline{[C]}_0 = C_0 \sqrt[n]{\frac{c}{k}} \, ,$$

where c is defined in Table 3. This approximation is valid until

$$k \left(\frac{[C]}{[C]_0} \right)^n \approx c \Longleftrightarrow [C] = \overline{[C]}_0,$$

When the concentration $\overline{[C]}_0$ is reached, the system may be simplified as

$$\frac{d[CE]}{dt} = (1+\sigma_C)\frac{d[C]}{dt} + \left[k_{fc}(1+\sigma_C)\overline{[C]}[E] - \frac{k_{fc}}{K_C}[CE] \right] \, , \qquad (13)$$

$$\frac{d[E]}{dt} = -\frac{\sigma_c}{1+\sigma_c}\frac{d[CE]}{dt} \, , \qquad (14)$$

$$\frac{d[C]}{dt} = -\left\{ k\left(\frac{\overline{[C]}}{[C]_0}\right)^n + c \right\} \frac{[CE]}{1+\sigma_C} \frac{K_{C/Eth}}{[Eth] + K_{C/Eth}} \, , \qquad (15)$$

where $\overline{[C]}$ and $\overline{[Eth]}$ are the average values over the time period considered. Combining the three equations (13-15) leads to

$$\frac{d^2[C]}{dt^2} + \left[\frac{K_{C/Eth}}{\overline{[Eth]} + K_{C/Eth}} \left\{ k\left(\frac{\overline{[C]}}{[C]_0}\right)^n + c \right\} + k_{fc}\sigma_C\overline{[C]} + k_{rc} \right] \frac{d[C]}{dt}$$

$$+ \frac{K_{C/Eth}}{\overline{[Eth]} + K_{C/Eth}} \left\{ k\left(\frac{\overline{[C]}}{[C]_0}\right)^n + c \right\} k_{fc}E_0\overline{[C]} = 0 \, . \quad (16)$$

The concentration may then be expressed as

$$[C] = \Gamma_1 e^{\alpha_1 t} + \Gamma_2 e^{\alpha_2 t} \, . \qquad (17)$$

Interval	$[C]_1$ (g/L)	$[C]_2$(g/L)	$\overline{[C]}$(g/L)	$\overline{[Eth]}$ (g/L)	α(g/L)	t_0 (g/L)
1	75	10	32.25	22	-0.033564	2.48
2	10	2	4.97	50	-0.077908	62.51

Table 4: Values used in the analytical approximation

In practice, one of the two roots (α_1, α_2) is very close to 0 and the other root is very negative. Neglecting the very negative root, the concentration of cellulose reduces to

$$[C] = \Gamma e^{\alpha(t-t_0)}$$

and the exponential decay of the previous section is retrieved. The average value $\overline{[C]}$ may then be evaluated as

$$\overline{[C]} = \frac{[C]_2 - [C]_1}{\ln\left(\frac{[C]_2}{[C]_1}\right)} \ ,$$

and $[C]_1$ and $[C]_2$ are cellulose concentrations at the beginning and end of the period considered. The corresponding values of $\overline{[Eth]}$ is estimated using chemical considerations at first and are then adjusted to fit the numerical curve. For this second type of approximation, the cellulose is calculated over two intervals as indicated in Table 4. The corresponding curve may be seen on Figure 3 As could be expected, the numerical and approximated curves are extremely close at the two extremities. This corresponds to the situation when the approximations and averages are the most appropriate. In the middle section, the curves decrease too fast at first and then too slowly. This is an expected consequence of averaging. Overall, with the values provided in Table 4, the cellulose concentration can be reasonably approximated without solving the complete system.
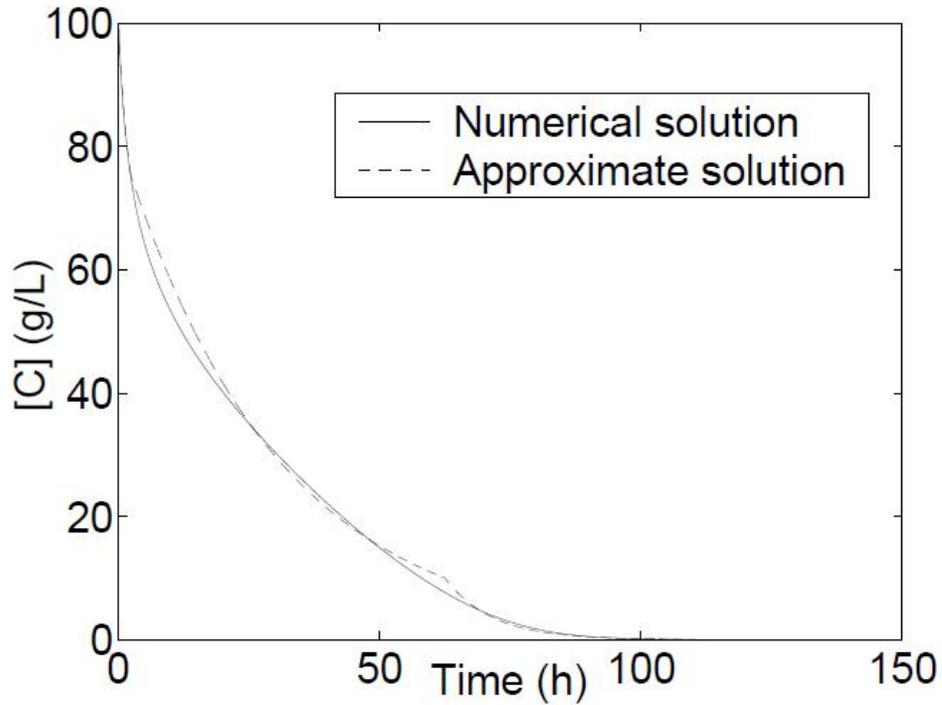
Figure 3: Numerical and approximate solutions for cellulose concentration

3   Fluid mechanics

Some fluid flow aspects of the process will now be investigated. The movements of the particles in the still tank are studied first and the flow of the mixture and the impeller are considered.

3.1   Cellulose particles

As already observed, the cellulose particles are tiny spherical wooden particles of diameter $d = 1$mm. They fall towards the bottom of the tank. The settling velocity can be estimated using Stokes' law [20] and Newton's Second Law:

$$m\frac{dv}{dt} = \Delta mg - 3\pi d\mu v \ , \tag{18}$$

where $m = \pi \rho_{cellulose} d^3/6$ is the mass of the particle, g denotes gravity and the effective mass is defined as

$$\Delta m = \pi \left(\rho_{cellulose} - \rho_{water} \right) \frac{d^3}{6} \ .$$

The dynamic viscosity and the densities of water and cellulose are respectively μ, $\rho_{cellulose}$ and ρ_{water}. Using Equation (18), the velocity may be calculated as

$$v = U_s \left(1 - e^{-t/\tau} \right) , \tag{19}$$

where the maximum settling velocity U_s and the typical time τ are defined as

$$U_s = \frac{\left(\rho_{cellulose} - \rho_{water} \right) g d^2}{18\mu} \ , \qquad \tau = \frac{\rho_{cellulose} d^2}{18\mu} \ .$$

Using typical values given in Table 5, the typical time is $\tau \sim 0.1$s. This value shows that the particles will reach the maximum settling velocity U_s in less than a second after they are introduced in the (still) tank. As the reaction progresses, the diameter d of the particles gets smaller and the value of τ diminishes. The particles will therefore always reach their maximum settling velocity less than a second after any forced movement is stopped. In the following, this transition period will be neglected and particles will be assumed to move at the constant velocity U_s. Using standard values detailed in Table 5, at the beginning of the process, particles move at the velocity $U_s = 0.3$m·s^{-1}: it takes the particles $\tau_{bottom} \sim 1$ minute to reach the bottom of the 18 metre high tank.

As the reaction advances, the diameter d of the particles diminishes and the particles will travel more slowly. The velocity U_s may be expressed as a function of the concentration $[C]$. Assuming the particles are always well mixed and that they remain spherical, the concentration of cellulose may be expressed as

$$[C] = \frac{m}{V} = \frac{\rho_{cellulose} \pi N d^3}{6V} \ , \tag{20}$$

where N is the number of particles in the solution and V is the volume of the tank. Using the concentration $[C]_0$ at $t = 0$, Equation (20) becomes

$$[C] = [C]_0 \frac{d^3}{d_0^3} \implies d = d_0 \left(\frac{[C]}{[C]_0} \right)^{1/3} \ .$$

The settling velocity may then be written:

$$U_s \ = \ \frac{\left(\rho_{cellulose} - \rho_{water} \right) g d_0^2}{18\mu} \left(\frac{[C]}{[C]_0} \right)^{2/3} = U_0 \left(\frac{[C]}{[C]_0} \right)^{2/3} \ . \tag{21}$$

Δm	Effective mass		kg
$\Delta \rho$	Effective density	600	kg·m^{-3}
μ	Dynamic viscosity	10^{-3}	kg·m^{-1}·s^{-1}
$\rho_{Cellulose}$	Density of cellulose	1600	kg·m^{-3}
ρ_{Water}	Density of water	1000	kg·m^{-3}
C	Concentration of cellulose		kg·m^{-3}
D	Diameter of the tank	9	m
N	Number of cellulose particles		
U_s	Settling velocity		m·s^{-1}
V	Volume of the tank	1000	m^3
d	Diameter of the cellulose spheres		m
g	Gravity	9.8	m·s^{-2}
t	Time		s
0	Value at $t = 0$		

Table 5: Typical value for the fluid flow

Using the results of the previous section, at the end of the process, it would take three to four hours for a particle to reach the bottom of the tank. Mixing will therefore have to take place during the entire length of the process to guarantee a uniform distribution of the particles in the fluid. It could only be switched off for the last few hours. Equation (21) may be combined with the analytical solution for cellulose concentration calculated in the previous section. This will be used to evaluate a minimum rotational speed for the impeller. This result may be obtained by studying the movement of the particles due to the impeller. This will now be investigated.

3.2 Fluid flow

Fluid movements in the tank will be very difficult to simulate. When the impeller in switched on, the upward flow should be able to compensate for the settling velocity and push the particles up to the top of the tank. A typical fluid velocity should be at least $U = 0.3$m·s^{-1}. With a typical length $L = 1$m, the Reynolds number can therefore be estimated as

$$Re = \frac{\rho U L}{\mu} = \mathcal{O}\left(10^6\right) \ .$$

Even if the settling velocity decreases significantly, the minimal flow required to prevent a particle accumulation at the bottom of the tank is going to be extremely

turbulent. The average velocities in the tank will also depend of the type of impeller used. Average velocity values for various turbines may be seen in [21]. Depending on the characteristics of the turbine, the (average) flow in the tank will vary significantly. Figure 4 shows idealised flows for two typical turbine geometries [21, 22].
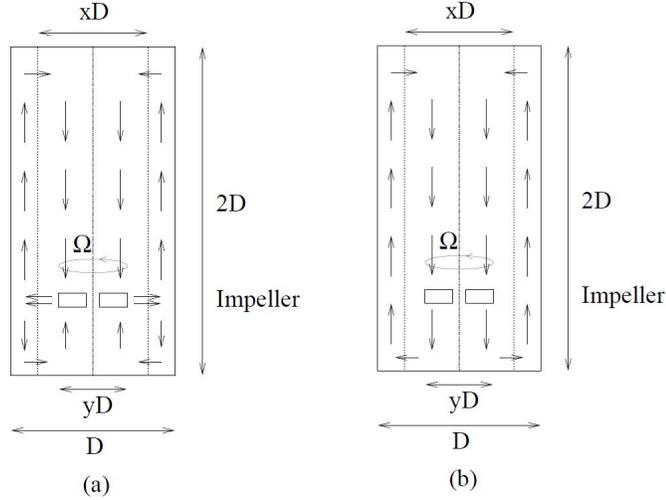
Figure 4: Idealised flows for two impeller designs

The radial flow in the impeller is shown in Figure 4a. In this case, the impeller generates a radial fluid flux that splits close to the wall. Part of the fluid flows down the wall towards the bottom of the tank while the rest flows towards the top. In the right half of the tank, fluid flows in a clockwise direction below the impeller and anti-clockwise above it. The axial impeller shown in Figure 4b generates a single cycle in the complete half tank in the anti clockwise direction. In the idealised situations described here, the width of the layer along the wall is assumed to be constant. This model could become closer to reality, particularly if several impellers were added on the vertical axis. This would add vertical movement in zones close to the top of the tank where one expects a much slower velocity with the present design.

The upwards velocity close to the tank wall should compensate the settling velocity of the particles. For both designs, the average velocity in the near-wall zone may be expressed as

$$V = \frac{Q}{\pi D^2 \left(1 - x^2\right)} \ ,$$

(22)

where Q denotes the fluid flow in the zone close to the wall, $D = 9$m is the diameter of the tank and $x \in [0\ 1]$ represents the ratio between the internal diameter of the boundary zone near the wall and the tank diameter. This value should be evaluated experimentally. The flux Q is highly dependent on the impeller design. Its value may be estimated using the non-dimensional number Ω_Q defined as

$$\Omega_Q = \frac{Q}{\Omega\,(yD)^3} \ ,$$

where Ω is the rotation speed of the impeller [22]. The value for this non-dimensional number was measured experimentally for various designs. For a radial flow impeller, Rushton type with 4 blades, sensible values could be [22]

$$x = 0.5 \ , \qquad y = 1/3 \ , \qquad \Omega_Q = 0.85 \ .$$

The value for parameter x is a guess but is most certainly an under-estimate. Assuming $r = 50\%$ of the radial flux created by the impeller moves upwards when reaching the wall, the minimum rotation speed of the impeller can be estimated as

$$\Omega > \frac{\pi U_s\left(1 - x^2\right)}{\Omega_Q Dry^3} \sim 5\text{rad} \cdot \text{s}^{-1} \ . \tag{23}$$

This corresponds to about 50 rotations per minute at the beginning of the reaction.

Possible values for an axial flow impeller, pitch blade type with 4 blades are [22]

$$x = 0.5 \ , \qquad y = 1/3 \ , \qquad \Omega_Q = 0.75 \ .$$

Here again, the value for x is an under-estimate. This set of values leads to

$$\Omega > \frac{\pi U_s\left(1 - x^2\right)}{\Omega_Q Dy^3} \sim 2.8\text{rad} \cdot \text{s}^{-1} \ , \tag{24}$$

which corresponds to 27 rotations per minute at the beginning of the reaction.

In both cases, the value of Ω is an estimate of the rotation velocity required to guarantee that particles are able to travel up in the tank. This value might not be sufficient to achieve good mixing, the rotation speed necessary to achieve this goal and the time it takes to do it may be measured experimentally. As could be expected, the axial flow is much more efficient than the radial flow and should be favoured. The rotation values for both cases will vary as the chemical reaction evolves. Formulae (23-24) can be combined with the settling velocity formula (21) and the approximate expressions for cellulose concentration calculated in Section 2 to show the evolution of minimal rotation requirements.

h
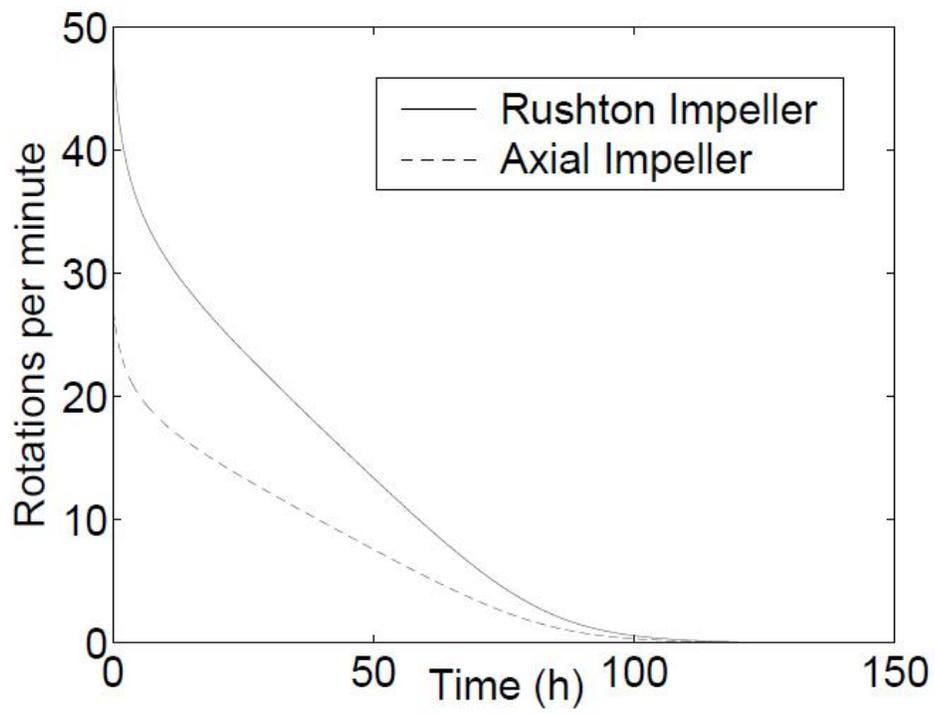
Figure 5: Number of rotations necessary for each type of impeller

As could be expected, the minimal rotation requirement decreases with time for both types of impellers, see Figure 5. For the first few hours, the axial type impeller is the less demanding but this advantage diminishes with time. After 4 days, the two types are equivalent and there is hardly any need to rotate the impeller. For too small rotation speeds, the mixing will most certainly not occur but the mixing should be much easier at higher speed.

The estimates in this section are calculated using values available on test tanks very much smaller than what is anticipated for the industrial production. Scaling up the values can provide very misleading results [22]. The results of this section therefore only provide a crude approximation of what would be the minimum requirements for the mixing in the tank.

4   Conclusion and future work

This study investigated various aspects of bio-fuel production:

- The chemical aspect of this problem was investigated first. Two models were considered. The two approaches lead to an exponential decay of cellulose concentration. The numerical and approximate solutions compare well and when necessary, the approximate solution may be used.

- The movements of particles in the tank were then studied when the impeller is off first and then the impeller is switched on. The settling velocity of the cellulose particles is related to cellulose concentration and minimum impeller rotation speeds were determined for different types of impellers. The results indicate that only minimum rotations of the impeller will be necessary after 4 days. These results are calculated using many approximations and should only be considered as indications of the tendency.

Experimental work would give appropriate values for all the parameters used in the present study. These experiments will be necessary as many assumptions were necessary to build the models.

Acknowledgements

References

[1] Luque, R., Herrero-Davila, L., Campelo, J.M., Clark, J.H., Hidalgo, J.M., Luna, D., Marinas, J.M. and Romero, A.A. Biofuels: a technological perspective. *Energy and Environmental Science,* **1** (2008), 542-564.

[2] Balat, M. and Balat, H. Recent trends in global production and utilization of bio-ethanol fuel. *Applied Energy,* **86** (2009), 2273-2282.

[3] Hahn-Hägerdal, B., Galbe, M., Gorwa-Grauslund, M.F., Lidén, G. and Zacchi, G. Bio-ethanol - the fuel of tomorrow from the residues of today. *Trends in Biotechnology,* **24** (2006), 549-556.

[4] Di Lucia, L. and Nilson, L.J. Transport biofuels in the European Union: The state of play. *Transport Policy* **14** (2006), 533-543.

[5] Balat, M., Balat, H. and Öz, C. Progress in bioethanol processing. *Progress in Energy and Combustion Science,* **34** (2008), 551-573.

[6] Taylor, M.P., Eley, K.L., Martin, S., Tuffin, M.I., Burton, S.G. and Cowan, D.A. Thermophilic ethanologenesis: future prospects for second-generation bioethanol production. *Trends in Biotechnology,* **27** (2009), 398-405.

[7] von Blotnitz, H. and Curran, M.A. A review of assessments conducted on bio-ethanol as a transportation fuel from a net energy, greenhouse gas and environmental life cycle perspective. *Journal of Cleaner Production,* **15** (2007), 607-619.

[8] Nordhoff, S. Editorial: food vs fuel - the role of biotechnology. *Biotechnology Journal,* **2** (2007), 1451.

[9] Tenenbaum, D.J. Food vs fuel: diversion of crops could cause more hunger. *Environmental Health Perspectives,* **116** (2008), A254-A257.

[10] Banerjee, S., Mudliar, S., Sen, R., Giri, B., Satpute, D., Chakrabarti, T. and Pandey, R.A. Commercializing lignocellulosic bioethanol: technology bottlenecks and possible remedies. *Biofuels, Bioproducts and Biorefining Biofpr,* **4** (2010), 77-93.

[11] Mtui, G.Y.S. Recent advances in pretreatment of lignocellulosic wastes and production of value added products. *African Journal of Biotechnology,* **8** (2009), 1398-1415.

[12] Farrell, A.E., Plevin, R.J., Turner, B.T., Jones, A.D., O'Hare, M. and Kamme, D.M. Ethanol can contribute to energy and environmental goals. *Science,* **311** (2006), 506-508.

[13] Margeot, A., Hahn-Hägendal, B., Edlund, M., Slade, R. and Monot, F. New improvements for lignocellulosic ethanol. *Current Opinion in Biotechnology,* **20** (2009), 372-380.

[14] Abdel-Banat, B.M.A., Hoshida, H., Ano, A., Nonklang, S and Akada, R. High-temperature fermentation: how can processes for ethanol production at high temperatures become superior to the traditional process using mesophilic yeast? *Applied Microbiology and Biotechnology,* **85** (2010), 861-867.

[15] Chang, V.S. and Holtzapple, M.T. Fundamental factors affecting biomass enzymatic reactivity. *Applied Biochemistry and Biotechnology,* **84** (2000), 5-37.

[16] Kim, S. and Holtzapple, M.T. Effect of structural features on enzyme digestibility of corn stover. *Bioresource Technology,* **97** (2006), 587-591.

[17] Zhou, J., Wang, Y.H., Chu, J., Luo, L.Z., Zhuang, Y.P. and Zhang, S.L. Optimization of cellulase mixture for efficient hydrolysis of steam-exploded corn stover by statistically designed experiments. *Bioresource Technology,* **100** (2009), 819-825.

[18] South, C.R., Hogsett, D.A.L. and Lynd, L.R. Modeling simultaneous saccharification and fermentation of lignocellulose to ethanol in batch and continuous reactors. *Enzyme and Microbial Technology,* **17** (1995), 797-803.

[19] Shao, X., Lynd, L., Wyman, C. and Bakker, A. Kinetic modeling of cellulosic biomass to ethanol via simultaneous saccharification and fermentation: Part i, accomadation of intermittent feeding and analysis of staged reactors. *Biotechnology and Bioengineering,* **102** (2009), 59-65.

[20] Batchelor, G.K. *An Introduction to Fluid Mechanics.* Cambridge University Press, 2005.

[21] Ranade, V.V., Tayalia, Y. and Krishnan, H. Cíd predictions of flow near impeller blades in baffled stirred vessels: assessment of computational approach. *Chemical Engineering Communications,* **189** (2002), 895-922.

[22] Oldhue, J.Y. *Fluid Mixing Technology* . McGraw-Hill, New York, 1983.